Accepted Manuscript

Fluid diffusion in cracked composite laminates – Analytical, numerical and experimental study

Abedin Gagani, Andreas T. Echtermeyer

PII: S0266-3538(17)33031-2

DOI: 10.1016/j.compscitech.2018.03.025

Reference: CSTE 7143

To appear in: *Composites Science and Technology*

Received Date: 16 December 2017

Revised Date: 22 February 2018

Accepted Date: 17 March 2018

Please cite this article as: Gagani A, Echtermeyer AT, Fluid diffusion in cracked composite laminates – Analytical, numerical and experimental study, *Composites Science and Technology* (2018), doi: 10.1016/j.compscitech.2018.03.025.

Fluid Diffusion in Cracked Composite Laminates – Analytical, Numerical and Experimental Study

Abedin Gagani, Andreas T. Echtermeyer

Department of Mechanical and Industrial Engineering, Norwegian University of Science and Technology (NTNU), Trondheim, Norway

Corresponding author: abedin.gagani@ntnu.no +47 7359 3885

Abstract

Composite structural components are often subjected to service loads that cause cracks in off-axis layers, without compromising the load bearing capability of the structure. In marine or humid environments fluid ingress in the material can be accelerated by the presence of such cracks, leading to further strength degradation.

Several studies have been dealing with the effect of cracks on fluid diffusion in composites, sometimes with contradictory results. In this work the difference between cracks on the external and internal plies of the laminate has been addressed both experimentally and analytically, showing that the first ones have a strong influence on diffusivity, while the second have a negligible effect

Keywords: hygrothermal effect; crack; modelling; finite element analysis (FEA); fluid diffusion.

List of symbols

c	Moisture content
c_i	Length of i-th crack
C_i, D_j, E_k	1-D terms of 3-D solution of diffusion equation
c_{op}	Crack opening

D_{11}, D_{22}, D_{33}	Composite anisotropic diffusion constants
D_c^1	Equivalent diffusivity inside the crack in direction 1
D_c^3	Equivalent diffusivity inside the crack in direction 3
D_{H2O}	Water diffusion constant
h	Laminate thickness
l	Representative volume element length
l_c, l_i	Length of crack and length of cracks interruption
L	Laminate length
p	Number of cracks
$m_{composite}$	Composite sample mass
$M_{eq}^{composite}$	Composite sample mass increase at equilibrium
$M_{eq}^{cracked}$	Cracked composite sample mass increase at equilibrium
m_{water}	Water mass
n	N° of plies in the laminate
$n_{90°}$	N° of 90° plies in the laminate
t	Time
w	Width
x, y, z	Cartesian coordinate system
$\rho_{composite}$	Composite density
ρ_{water}	Water density
ρ_w	Crack density

1. Introduction

Multidirectional composite laminates are used in many structural applications where they are immersed in water or exposed to humid environment, like marine and offshore industry [1], aircraft industry and wind energy industry [2]. Multidirectional laminates subjected to unidirectional static or fatigue loadings, typically crack in the off-axis plies; in the case of a cross-ply laminate, cracks can appear only in the 90° plies.

Fluid diffusion in composites is an anisotropic phenomenon, for orthotropic laminates three diffusivities are necessary. These constants can be measured by weightgain measurements of immersed samples having different fiber orientation [3]. Using these diffusion constants, the water uptake of a cracked laminate can be predicted.

The experimental results available in the literature report different scenarios. In some cases, cracks have been reported to accelerate apparent diffusivity greatly [4, 5], while in others negligible effect was observed [6]. In **Table 1** an overview of the studies present in the literature about fluid diffusion in multidirectional pre-cracked laminates is reported along with the apparent diffusion ratio of cracked material vs. un-cracked material.

Table 1
Overview of diffusion experiments in pre-cracked composites

Reference	Material	Layup	$D_{cracked}/D$
Suri & Perreux [5]	GF/Epoxy	$[+55/-55]_s$	2.53
Lundgren & Gudmundson [6]	GF/Epoxy	$[0_2,90]_s$	1.04
		$[0_2,90_2,0]_s$	1.03
		$[0_4,90_2]_s$	1.07
		$[(0_2,90_2)_2,0]_s$	1.04
		$[0_4,90_4,0_2]_s$	1.11
		$[0_8,90_4]_s$	1.15
Roy and Bandorawalla [4]	GF/Epoxy	$[0/90/0/90]_s$ Woven	2.23
Present study	GF/Epoxy	[0/90/0]	1.11
		[90/0/90]	1.29

It is possible to observe a trend from the results reported in **Table 1**: samples with 0° layers on the outer surfaces show low diffusion increase when cracked, while samples having off-axis layers on the outer surfaces show higher diffusion increase when cracked. The cracks in the most external layers of the laminate seem to have a higher effect on diffusion than the cracks on the internal layers.

The only apparent exception is the one reported in [4], however this study dealt with satin weave layers, where cracks can appear in all layers, while in the other references unidirectional layers are studied, which contain cracks only in the off-axis plies.

Based on these considerations, in the present work [0/90/0] and [90/0/90] laminates have been mechanically loaded in the axial (0°) direction to four strain levels: ε = 0 %, ε = 1 %, ε = 1.5 % and ε = 2 %; to verify this hypothesis. An analytical model and a finite element model, based on change of boundary conditions (BCs) in the diffusion equation due to the presence of cracks is used. The increase of weight due to the cracks filling with water is also modelled. The different behaviour of cracks on internal and external layers is caused by their discontinuous shape. This effect is explained theoretically using a mono-dimensional fluid diffusion analysis. A good agreement between the experimental results and both analytical and finite element (FE) predictions was obtained.

2. Material and methods

2.1. Materials

A glass fiber/epoxy composite laminate has been manufactured using vaacum assisted resin transfer molding (VARTM). The matrix was Hexion Epikote^{TM} Resin RIMR135 mixed with Epikure^{TM} Curing Agent MGS RIMH134 with a mixing ratio of 100:30 by weight. The fibers were HiPer-tex UD glass fibers from 3B. Curing was performed at room temperature for 24h and post-curing in a ventilated oven at 80˚C for 16 h.

The volume fraction of the laminate was obtained by matrix burnoff test, resulting in 54.2 %. The density of the samples was 1.93 g/cm^3. Twenty [0/90/0] and twenty [90/0/90] tensile samples, were cut using a water-cooled diamond saw to 230 x 30 mm. Sample thickness was 2.7 mm. The material's mechanical properties have been characterized in previous studies [7]. The strain to failure of the UD laminate is 2.4 % in fiber direction and 0.4 % in transverse direction.

2.2. Experimental methods

Cracks were introduced into the samples by loading the coupons using an Instron 8800 tensile machine with a 100kN loadcell under displacement control. Three values of strain were chosen to obtain different crack densities on the samples, avoiding complete failure: ε = 1%, 1.5% and 2%. A set of samples for each layup was not loaded, to provide a reference for the un-cracked material diffusivity.

Fig.1 reports the dimension of the tensile samples. From each tensile coupon, a cracked diffusion sample was obtained from the central part, far from the tabs. The samples were cut using a circular water-cooled diamond saw, resulting in dimensions: 48.5 x 30 x 2.5 mm.

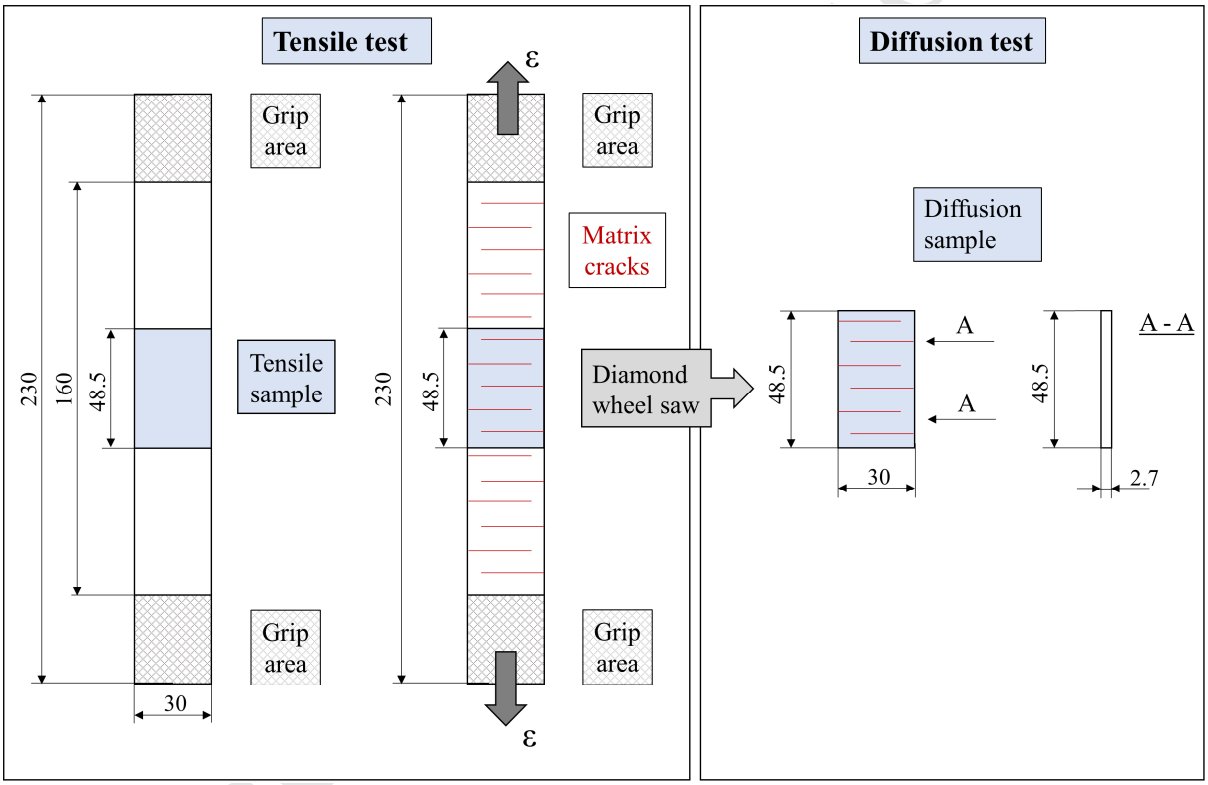

Fig. 1. Dimensions of the tensile coupons and of the diffusion sample.

Five replicates were loaded for each strain; four were conditioned after loading and one was cut, grinded, polished and analysed with an optical microscope, in order to provide more information about the crack morphology.

From the visual inspection of the samples before and after the test using translucency, **Fig. 2**, it was possible to measure the length of each crack, c_i. Cracks appear as horizontal lines when

uniaxial load is applied, **Fig. 2 (c, d, e)**. The matrix cracks developed only in the 90° plies. Due to the translucent nature of the epoxy the cracks could also easily be seen inside the laminate.

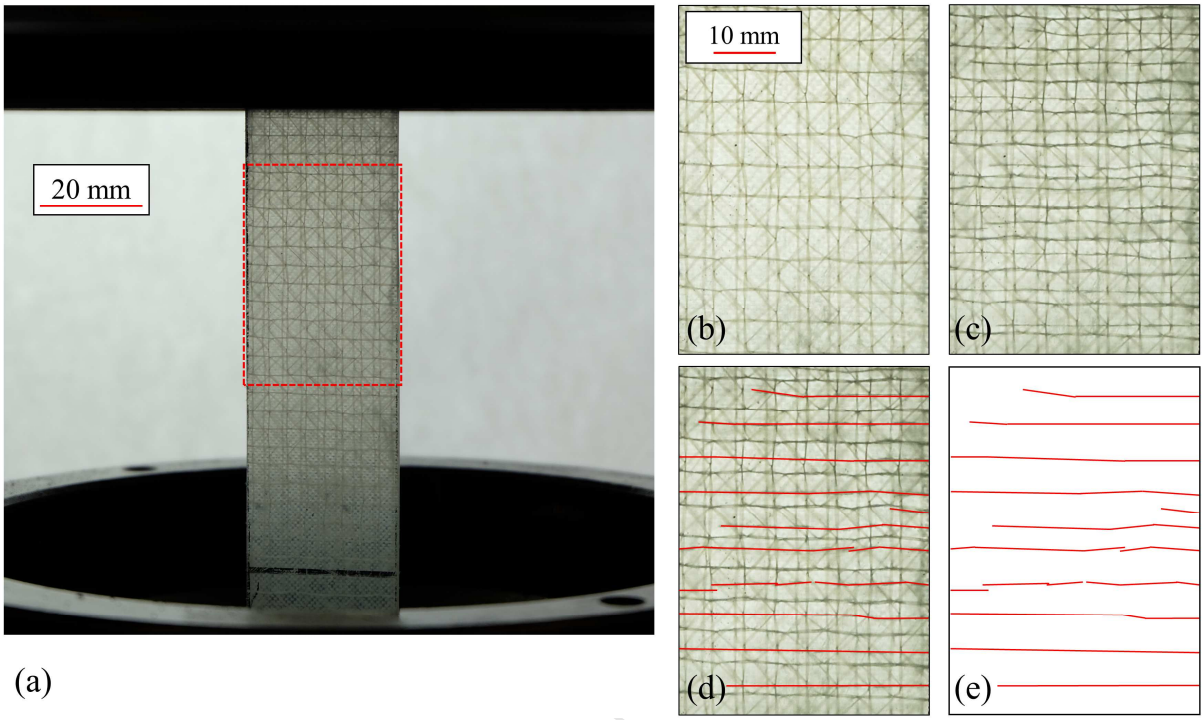

Fig. 2. (a) Tensile loading of [0/90/0] sample. (b) Sample before loading. (c) Sample after loading. (d) Cracks are highlighted with red lines. (e) cracks array obtained and used for calculation of ρ_w.

The weighted crack density, for a cross ply laminate, was then computed as follows [8, 9]:

$$\rho_w = \frac{\sum_{i=1}^{p} c_i}{w\,L} \qquad (1)$$

where c_i is the length of each crack, w the width of the laminate and L is the length of the laminate. Defining a weighted crack density allows considering that cracks do often not span over the entire thickness of the laminate. The measurements were further confirmed by the optical microscope analysis of the sample analysed with the optical microscope per each set. Crack densities obtained experimentally are reported in **Fig.3**.

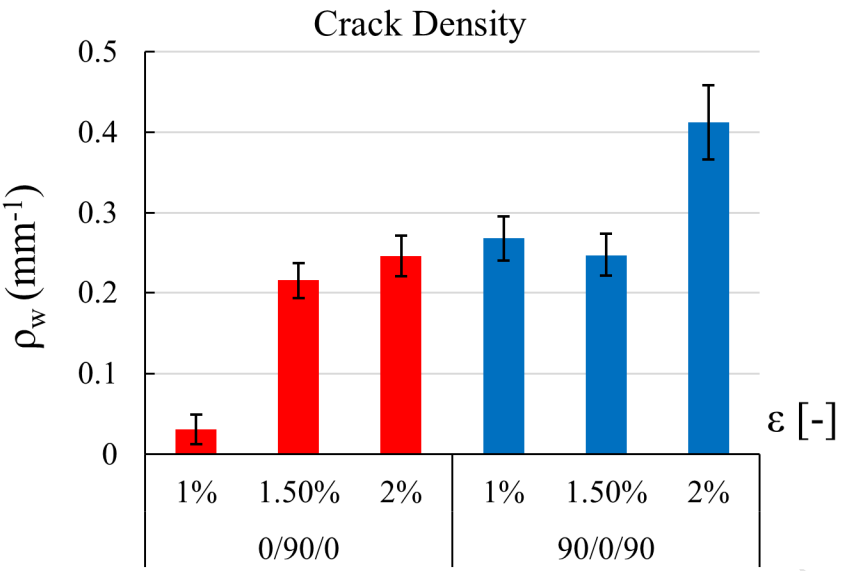

Fig. 3. Crack densities for [0/90/0] and [90/0/90] samples. Each point is the average of 4 measurements

Fig. 4 (a) and **(b)** shows optical micrographs of transverse cracks in [0/90/0] and [90/0/90] laminates. Cracks extend over the entire thickness of the layer. It can be also noticed that the cracks in the [90/0/90] laminate appear thicker than the cracks in the [0/90/0] laminate. This aspect can cause a difference in the final amount of water absorbed by the material; it was therefore decided to measure crack opening by means of microscope analysis. The average crack opening, obtained from 520 measurements, was:

- 5.24 μm ± 1.82 μm in the [90/0/90] laminates,
- 2.90 μm ± 1.00 μm in the [0/90/0] laminates.

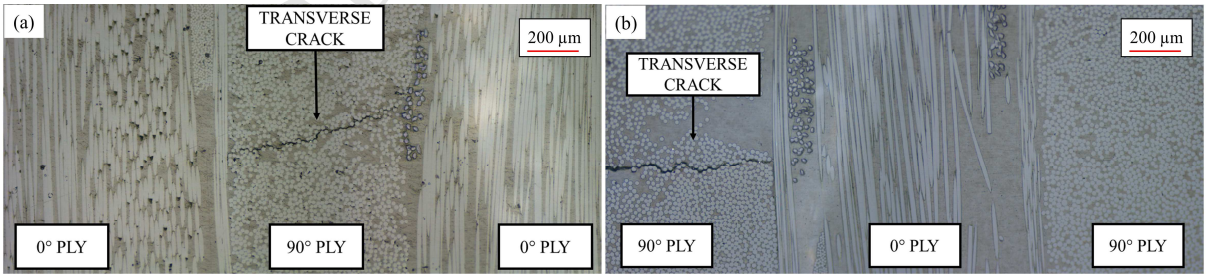

Fig. 4. Optical micrograph of: (a) [0/90/0] cracked sample; (b) [90/0/90] cracked sample.

Fig.2 indicates that most cracks seem to cross the entire width of the specimen. However, a closer inspection by microscope, **Fig.5**, reveals that the wide cracks are actually an accumulation of disconnected shorter cracks. This aspect needs to be considered in the

model, because the continuous cracks in the width direction give a very different diffusion behaviour that discontinuous cracks.

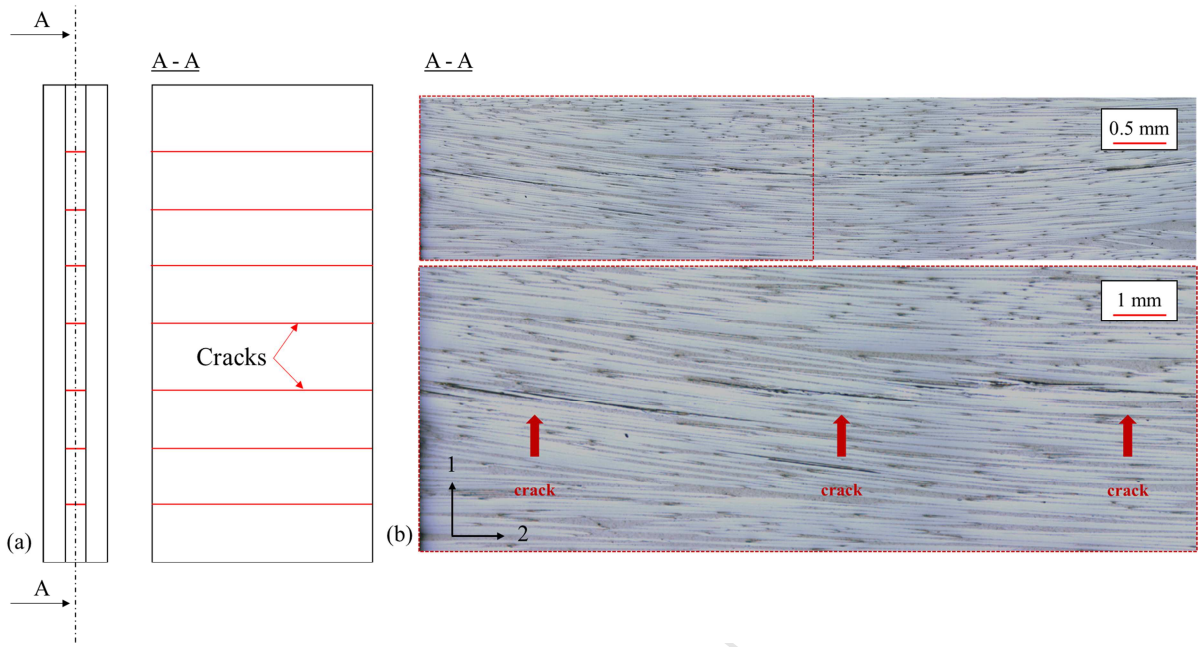

Fig. 5 Matrix crack in the sectioned 90° ply of a [0/90/0] cracked laminate: (a) Scheme, (b) Section with laminate global coordinate system.

Samples were dried for 72 hours in an oven at 40˚C and their weight was recorded daily, until stabilization. The samples were subsequently conditioned in a bath with distilled water at 60˚C ± 1 ˚C. This temperature provides a convenient acceleration of the test, compared to room temperature, without activating additional mechanisms that could influence the water uptake process [2, 10], especially close to the glass transition temperature of the resin, which is 84.7°C for the epoxy tested in this study [11]. Water was refilled regularly in order to provide always distilled and uncontaminated water.

Weighing of the specimens was performed extracting them from the conditioning chamber, drying their surface with a dry cloth and weighing the samples with a Mettler Toledo AG204 DeltaRange scale (sensibility 0,1 mg). The weight was recorded and the weight increase was calculated according to the ATSM standard for composite fluid diffusion [12].

3. Analytical Model

An analytical model for weight gain prediction in cracked laminates, based on the principle of separation of variables, is presented here. The model deals with cross ply laminates, containing only 0° and 90° plies. The main modelling assumptions are:

- Fick's equations are assumed to govern the diffusion problem;
- The cracks are considered as empty volume, initially filled with air and able to host water proportionally to their volume;
- The cracks are assumed to be equally spaced, as shown in **Fig.2**. The presence of cracks causes a change in the fluid diffusion equation boundary conditions, since crack faces become exposed to water.

3.1. Moisture saturation content

For a laminate having n-plies and dimensions L, w, h: respectively length, width and thickness, the moisture equilibrium content at equilibrium is:

$$M_{eq}^{cracked} = M_{eq}^{composite} + \frac{m_{water}}{m_{composite}} \tag{2}$$

Where $M_{eq}^{cracked}$ is the moisture equilibrium content for the cracked laminate, $M_{eq}^{composite}$ is the moisture saturation content for the un-cracked laminate, m_{water} is the total mass of water that the cracks can absorb, and $m_{composite}$ is the mass of the dry laminate. It can be assumed that the mass of water inside the cracks is proportional to their volume:

$$M_{eq}^{cracked} = M_{eq}^{composite} + \frac{\rho_{water} \frac{h}{n} c_{op} \sum_{i=1}^{p} c_i}{\rho_{composite} L w h} \tag{3}$$

where ρ_{water} is water density, $\rho_{composite}$ is composite density, c_{op} is the crack opening, c_i is the length of the i-th crack, p is the total number of cracks, h is the sample thickness and n is the number of layers in the laminate. Rearranging the definition of crack density, Eq. (1):

$$\frac{\sum_{i=1}^{p} c_i}{w} = L \rho_w \tag{4}$$

Substituting Eq. (4) in Eq. (3), it is possible to predict the moisture saturation content of a cross-ply cracked laminate as a function of the crack density, ρ_w:

$$M_{eq}^{cracked} = M_{eq}^{composite} + \frac{\rho_{water}\, c_{op}\, \rho_w}{n\, \rho_{composite}} \quad (5)$$

3.2. Mono-dimensional analysis of fluid diffusion in surface cracks and internal cracks

With a procedure based on the one-dimensional Fick's first law [13], the difference between cracks in the internal plies and cracks on the external plies can be analysed. In the width direction of a laminate cracks have typically a non-continuous geometry, as shown in **Figs. 2, 5, 6**: the cracks present some interruptions in the width direction. This effect is important for [0/90/0] laminates, having cracks in the internal ply, since these channels are the only paths allowing quick water penetration in the sample, **Fig. 6 (b)**. For [90/0/90] laminates, having cracks in the external plies, the cracks are also non-continuous in the width direction. However, for this layup, the cracks extend through the whole ply thickness, reaching the laminate surface, and allowing an additional path for crack initial saturation, **Fig. 6 (c)**. It is possible to study the initial fluid diffusion in the cracks by modelling the crack as a rectangle having length equal to the crack length, hence ply width and height equal to the ply thickness.

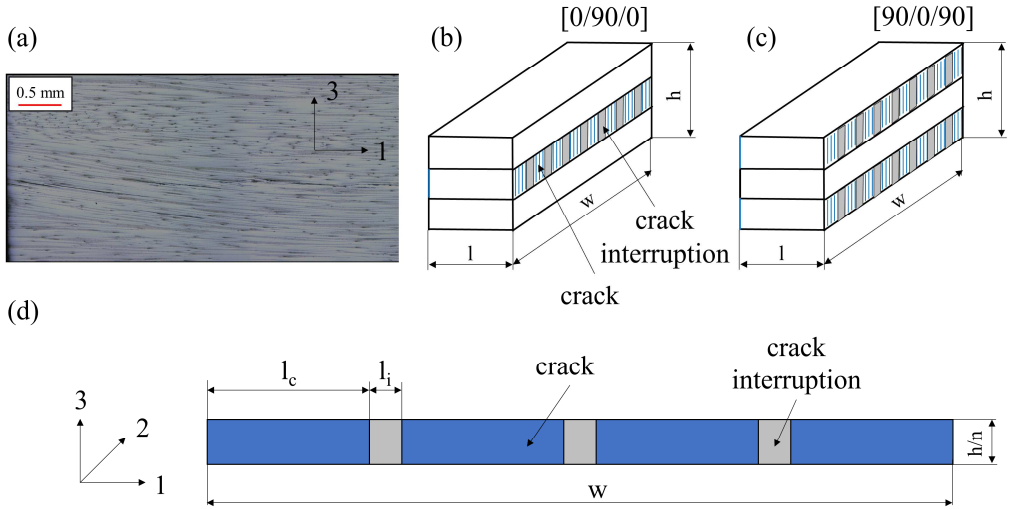

Fig. 6 (a) Optical micrograph of a cracked sample (b) scheme of a non-continuous crack in a [0/90/0] cracked laminate (c) scheme of a non-continuous crack in a [90/0/90] cracked laminate (d) 1-D diffusion model in crack

In laminates having cracks on external plies, like [90/0/90], fluid diffusion inside the crack occurs both in width and thickness direction: 1 and 3 directions in **Fig. 6 (d)**.

Fluid diffusion in the crack in direction 1 can be estimated using an equivalent diffusion model with crack and crack interruption placed in series. Diffusion in the crack occurs with a diffusivity equal to D_{H2O}, water diffusivity in air, while diffusion in the crack interruption occurs with a diffusivity D_{11}, composite diffusivity in direction 1. The equivalent diffusion in the crack in direction 1 can be obtained using a series connection of materials, based on Fick's 1st law:

$$\frac{l_c}{D_{H_2O}} + \frac{l_i}{D_{11}} = \frac{(l_c+l_i)}{D_C^1} \tag{6}$$

where D_C^1 is the equivalent water diffusivity in the crack in direction 1, D_{11} the diffusivity in the composite in direction 1, D_{H20} the water diffusivity in air, l_c is average crack length and l_i the average crack interruption length, shown in **Fig. 6 (d)**. D_C^1 can be expressed as:

$$D_C^1 = (l_c + l_i)\frac{D_{H_2O}\, D_{11}}{l_c\, D_{11} + l_i\, D_{H_2O}} = (l_c + l_i)\frac{D_{11}}{l_c \frac{D_{11}}{D_{H_2O}} + l_i} \tag{7}$$

From **Table 3**, D_{11}= 0.01598 mm^2/h and $D_{H20} \approx$ 106108 mm^2/h, the ratio $D_{11}/D_{H20} = 1.51\ 10^{-7}$ and can be considered null. Furthermore, since l_i and l_c have the same order of magnitude, the ratio $(l_c+l_i)/l_i$ can be assumed equal to 1. For an estimation of diffusivity in the crack, Eq. (7) can be simplified:

$$D_C^1 \approx \frac{l_c+l_i}{l_i} D_{11} \approx D_{11} \tag{8}$$

It is possible to conclude the fluid diffusion in a crack in an external layer in direction 1 occurs with a diffusivity close to the diffusivity of the composite material in direction 1: D_{11}, hence not providing an increase of diffusivity compared to the reference un-cracked material.

Fluid diffusion in the crack in direction 3 can be estimated using a parallel connection of materials, based on Fick's 1st law, [14]:

$$D_C^3(l_c + l_i) = D_{H2O} l_c + D_{33} l_i \tag{9}$$

$$D_C^3 = \frac{D_{H2O} l_c + D_{33} l_i}{(l_c + l_i)} = \frac{l_c + \frac{D_{33}}{D_{H2O}} l_i}{\frac{(l_c + l_i)}{D_{H2O}}} \quad (10)$$

From **Table 3**, D_{33}= 0.0036 mm^2/h and $D_{H20} \approx$ 106108 mm^2/h, the ratio D_{33}/D_{H20} = 3.39 10^{-8} and can be considered null. Furthermore, since l_i and l_c have the same order of magnitude, the ratio $l_c/(l_c+l_i)$ can be assumed equal to 1. For an estimation of diffusivity in the crack, Eq. (10) can be simplified:

$$D_C^3 \approx \frac{l_c}{l_c + l_i} D_{H2O} \approx D_{H2O} \quad (11)$$

Fluid diffusion in a crack in an external layer, in direction 3, occurs with a diffusivity close to the diffusivity of water in air, D_{H2O}, hence providing a strong increase of diffusivity compared to the reference un-cracked material.

For layups having cracks on external plies, diffusion takes place in direction 1 with a diffusivity close to the reference composite diffusivity, and in direction 3 with a diffusivity close to the water diffusivity in air; which is much greater than the previous one. This analysis suggests that cracks on external plies fill immediately with fluid when a cracked laminate is immersed in water.

In laminates having cracks on internal plies, fluid diffusion inside the crack cannot take place in direction 3, but occurs only in direction 1, therefore it can be estimated using an equivalent thermal model, with crack and crack interruption in series [14], as shown in Eqs. (6-7).

Fluid diffusion in internal cracks in direction 1 can be estimated as in Eq. (8):

$$D_C^1 \approx D_{11} \quad (12)$$

Since fluid diffusion in the crack in an internal ply occurs at the same rate as fluid diffusion in the composite, the presence of the crack can be neglected in terms of diffusivity, and the composite can be modelled as un-cracked. In this case, the cracks behave as an “empty volume”, they don’t saturate immediately as in the previous case, however when they saturate they lead to a higher moisture saturation content than for an un-cracked laminate.

3.3.Diffusivity prediction

Fick's second law for diffusion in orthotropic materials is [6, 15]:

$$\frac{\partial^2 c}{\partial t^2} = D_{11}\frac{\partial c}{\partial x} + D_{22}\frac{\partial c}{\partial y} + D_{33}\frac{\partial c}{\partial z} \tag{13}$$

where c (*x*, *t*) is water concentration, *t* is time, *x, y* and *z* space coordinates and D_{11}, D_{22} and D_{33} diffusivities in directions 1,2 and 3 respectively.

For an orthotropic plate, having length L, width w and thickness h, the solution of the three-dimensional anisotropic diffusion equation is [15]:

$$M(t) = M_{eq}^{composite}\left[1 - \left(\frac{8}{\pi^2}\right)^3 \sum_{i=1}^{\infty}\sum_{j=1}^{\infty}\sum_{k=1}^{\infty} C_i \cdot D_j \cdot E_k\right] \tag{14}$$

where the terms C_i, D_j and E_k consider 1-D mass flow in thickness direction, length direction and width direction.

$$C_i = \frac{1}{(2i-1)^2} e^{-(2i-1)^2\left(\frac{\pi}{h}\right)^2 D_{33}t} \tag{15}$$

$$D_j = \frac{1}{(2j-1)^2} e^{-(2j-1)^2\left(\frac{\pi}{L}\right)^2 D_{11}t} \tag{16}$$

$$E_k = \frac{1}{(2k-1)^2} e^{-(2k-1)^2\left(\frac{\pi}{w}\right)^2 D_{22}t} \tag{17}$$

For a cross-ply laminate having n-plies, of which $n_{90°}$-90° plies, the term dealing with diffusion through the thickness, C_i, remains unchanged, Eq. (15). The terms dealing with diffusion through the length and through the width of the laminate, D_j and E_k respectively, need to be modified as follows:

$$D_j = \frac{1}{(2j-1)^2} e^{-(2j-1)^2\left(\frac{\pi}{L}\right)^2 \frac{\left((n-n_{90°})D_{11}+n_{90°}D_{22}\right)}{n}t} \tag{18}$$

$$E_k = \frac{1}{(2k-1)^2} e^{-(2k-1)^2\left(\frac{\pi}{w}\right)^2 \frac{(n_{90°}D_{11}+(n-n_{90°})D_{22})}{n}t} \tag{19}$$

Eqs. (18-19) assume that for a cross-ply laminate, diffusion in length and width directions are a weighted average of the diffusivity of each ply. The validity of this assumption will be shown in the results section, comparing the analytical and the FE prediction.

Substituting Eqs. (5,18,19) in Eq. (14), the expression for the weight gain of an un-cracked cross-ply laminate becomes:

$$M(t) = M_{eq}^{composite}\left[1-\left(\frac{8}{\pi^2}\right)^3\sum_{i=1}^{\infty}\sum_{j=1}^{\infty}\sum_{k=1}^{\infty}\frac{1}{(2i-1)^2}e^{-(2i-1)^2\left(\frac{\pi}{h}\right)^2 D_{33}t}\cdot\right.$$

$$\left.\frac{1}{(2j-1)^2}e^{-(2j-1)^2\left(\frac{\pi}{L}\right)^2\frac{\left((n-n_{90^\circ})D_{11}+n_{90^\circ}D_{22}\right)}{n}t}\cdot\frac{1}{(2k-1)^2}e^{-(2k-1)^2\left(\frac{\pi}{w}\right)^2\frac{(n_{90^\circ}D_{11}+(n-n_{90^\circ})D_{22})}{n}t}\right] \quad (20)$$

For [0/90/0] laminates, having cracks in the internal plies, the cracks do not influence diffusion, but only moisture saturation content, as shown in the previous paragraph. The fluid diffusivity of the laminate with cracks in the internal ply can be predicted as follows:

$$M(t) = M_{eq}^{cracked}\left[1-\left(\frac{8}{\pi^2}\right)^3\sum_{i=1}^{\infty}\sum_{j=1}^{\infty}\sum_{k=1}^{\infty}\frac{1}{(2i-1)^2}e^{-(2i-1)^2\left(\frac{\pi}{h}\right)^2 D_{33}t}\cdot\right.$$

$$\left.\frac{1}{(2j-1)^2}e^{-(2j-1)^2\left(\frac{\pi}{L}\right)^2\frac{\left((n-n_{90^\circ})D_{11}+n_{90^\circ}D_{22}\right)}{n}t}\cdot\frac{1}{(2k-1)^2}e^{-(2k-1)^2\left(\frac{\pi}{w}\right)^2\frac{(n_{90^\circ}D_{11}+(n-n_{90^\circ})D_{22})}{n}t}\right] \quad (21)$$

The only difference between the weight gain expression for a cracked [0/90/0] laminate, Eq. (21), and an un-cracked [0/90/0] laminate, Eq. (20), is the moisture saturation content $M_{eq}^{cracked}$, which was defined is Eq. (5).

For a [90/0/90] laminate, having cracks in the external plies, the presence of cracks has a strong influence on diffusivity, as shown in the previous paragraph.

Since cracks fill almost immediately with water, the boundary conditions of the diffusion problem change. This aspect can be modelled by defining a Representative Volume Element (RVE) representing a portion of laminate between two adjacent cracks, **Fig. 7**. The RVE definition is based in the hypothesis of equally spaced cracks. The dimensions of the RVE are w, h and l. The terms w and h are the width and thickness of the laminate. The term l, RVE length, is a function of the crack density, as follows:

$$l = \frac{n_{90^\circ}L}{\rho_w L+1} \quad (22)$$

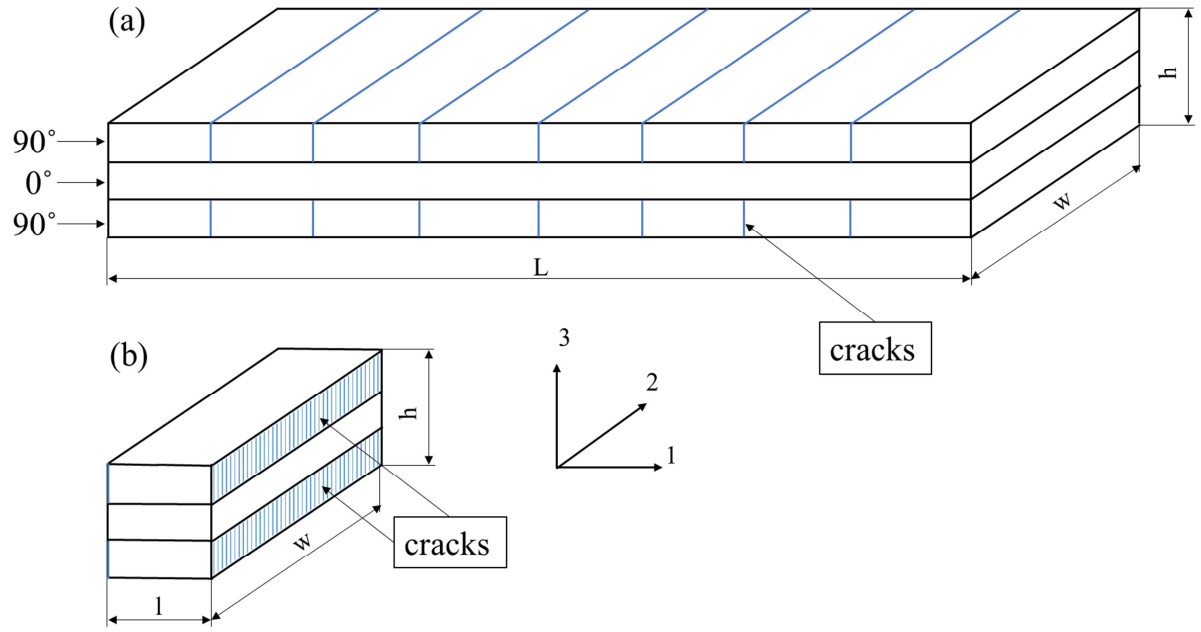

Fig.7. Laminate dimensions and dimensions of the RVE used for the derivation of the analytical solution

The dimensions of the RVE are reported in **Table 2**. The moisture saturation content of the laminate was measured from the weight gain curves of the un-cracked samples. The ply diffusion constants we also measured from the weight gain curves of the un-cracked samples, assuming transverse isotropy: $D_{22} = D_{33,}$ as verified experimentally by Rocha *et al.* [2], and a ratio between axial diffusion and transverse diffusion equal to the one measured in a previous study of the authors on the same material ($D_{11} = 4.44\ D_{33}$) [3]. These hypotheses allowed reducing the number of un-knowns from three to one, allowing identification of the orthotropic diffusion constants from the weight gain curve of the un-cracked samples using Eq. (20). The material properties used in the analytical and FE model are summarized in **Table 3**.

Table 2
Values of FE RVE lengths l [mm] for different applied strains

Layup	Undamaged (mm)	ε = 1 % (mm)	ε = 1.5 % (mm)	ε = 2 % (mm)
0/90/0	48.5	48.5	48.5	48.5
90/0/90	48.5	6.928	7.462	4.618

Table 3
Material properties used for the analytical and FE model. The properties refer to 60° distilled water.

Constituent	M_{eq} (-)	D_{11} (mm^2/h)	D_{22} (mm^2/h)	D_{33} (mm^2/h)
GF-Epoxy	0.93 %	0.01598	0.0036	0.0036
Crack	100 %	106 108	106 108	106 108

For the cracked [90/0/90] laminate, the three-dimensional orthotropic diffusion equation, Eq. (13), is solved considering that cracks do not extend through the whole thickness of the laminate; cracks do not go through 0° plies. This aspect is considered by modifying the term describing diffusion in the length direction of the RVE, D_j, where the 0° ply is not exposed to the fluid, while the 90° plies are exposed to fluid and have diffusivity D_{22}. The term D_j becomes then:

$$D_j = \frac{1}{(2j-1)^2} e^{-(2j-1)^2 \frac{\left(\frac{\pi}{l}\right)^2 n_{90^\circ} D_{22}}{n} t} \quad (23)$$

The weight gain for a cracked laminate becomes:

$$M(t) = M_{eq}^{cracked} \left[1 - \left(\frac{8}{\pi^2}\right)^3 \sum_{i=1}^{\infty}\sum_{j=1}^{\infty}\sum_{k=1}^{\infty} \frac{1}{(2i-1)^2} e^{-(2i-1)^2\left(\frac{\pi}{h}\right)^2 D_{33} t} \cdot \frac{1}{(2j-1)^2} e^{-(2j-1)^2 \frac{\left(\frac{\pi}{l}\right)^2 n_{90^\circ} D_{22}}{n} t} \cdot \frac{1}{(2k-1)^2} e^{-(2k-1)^2\left(\frac{\pi}{w}\right)^2 \frac{(n_{90^\circ} D_{11} + (n - n_{90^\circ}) D_{22})}{n} t}\right] \quad (24)$$

Where $M_{eq}^{cracked}$ is obtained from Eq. (5). Substituting Eq. (5) in the newly obtained Eq. (24), we obtain the weight gain prediction for a cracked laminate:

$$M(t) = \left(M_{eq}^{composite} + \frac{\rho_{water}\, \rho_w\, c_{op}}{n\, \rho_{composite}}\right) \left[1 - \left(\frac{8}{\pi^2}\right)^3 \sum_{i=1}^{\infty}\sum_{j=1}^{\infty}\sum_{k=1}^{\infty} \frac{1}{(2i-1)^2} e^{-(2i-1)^2\left(\frac{\pi}{h}\right)^2 D_{33} t} \cdot \frac{1}{(2j-1)^2} e^{-(2j-1)^2 \frac{\left(\frac{\pi}{l}\right)^2 n_{90^\circ} D_{22}}{n} t} \cdot \frac{1}{(2k-1)^2} e^{-(2k-1)^2\left(\frac{\pi}{w}\right)^2 \frac{(n_{90^\circ} D_{11} + (n - n_{90^\circ}) D_{22})}{n} t}\right] \quad (25)$$

4. Numerical Model

A water diffusion finite element model (FE) was developed using ABAQUS™ based on the same assumption used for the analytical model: Fickian orthotropic 3-D diffusion and equally spaced cracks modelled as empty volume.

Uniformly spaced cracks are modelled in the [90/0/90] laminate having crack opening: c_{op}, width equal to the samples total width: w, and thickness equal to ply thickness: h/n, **Fig.8**.

FE diffusion analysis is based on Fick's second diffusion law for anisotropic media [15]:

$$\frac{\partial^2 c}{\partial t^2} = D_{11}\frac{\partial c}{\partial x} + D_{22}\frac{\partial c}{\partial y} + D_{33}\frac{\partial c}{\partial z} \tag{26}$$

The influence of crack is considered by defining an appropriate RVE length, as in the analytical model, Eq. (22):

$$l = \frac{n_{90^\circ} L}{\rho_w L + 1} \tag{27}$$

where n_{90° is the number of 90° plies in the laminate.

The dimensions for the RVE used in the FE model are the same as the ones used in the analytical model and reported in **Table 2**. Material properties used for the FE model are also the same ones used for the analytical model and reported **Table 3**.

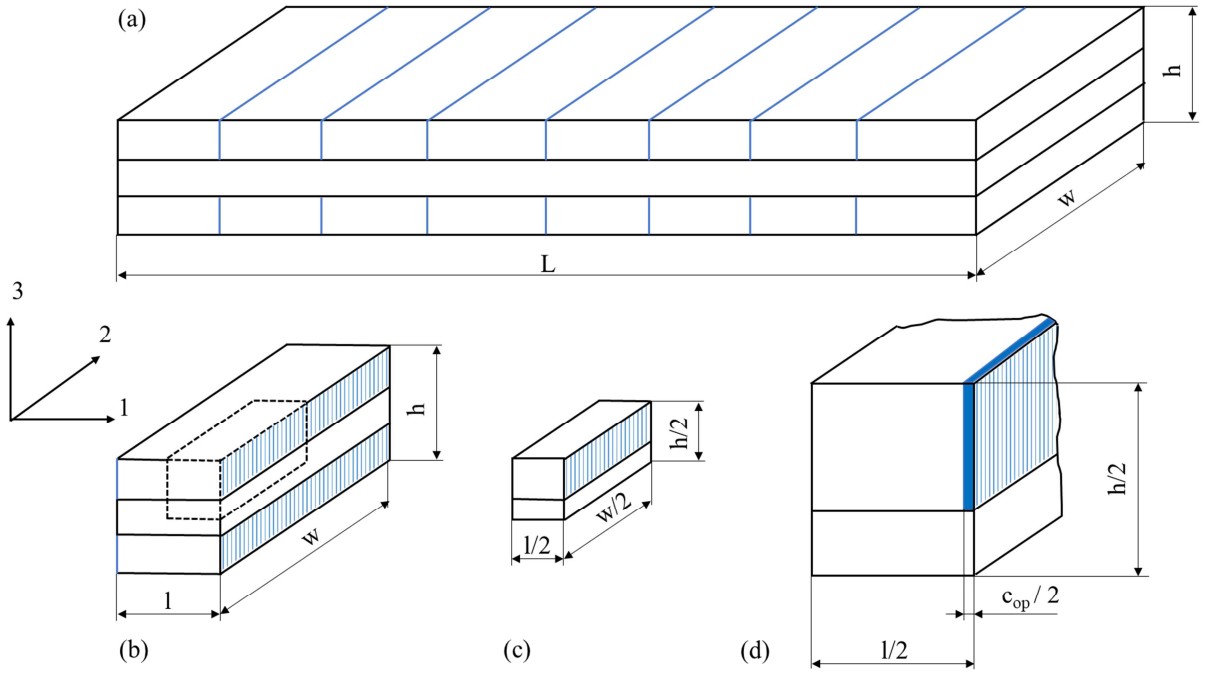

Fig. 8. (a) Scheme of a cracked 90/0/90 laminate (b) RVE for the cracked laminate. (c) 1/8 RVE obtained using 3 symmetry planes. (d) geometry and dimensions of the crack, extending over the whole width of the laminate.

Elements used are 3D 8-nodes elements for heat and mass transfer analyses (DC3D8), with an element size between 0.05 mm and 0.5 mm. This choice was based on a mesh

convergence analysis. The mesh of the FE model for the sample subjected to ε = 2 % is shown in **Fig. 9 (a)**. The boundary conditions used in the FE analysis, **Fig. 9 (b)**, are:

- three planes of symmetry, according to 1/8 geometric symmetry, **Fig. 8(c)**;
- water exposure to both top and lateral surface of the RVE, representing exposure of laminate faces and edges.

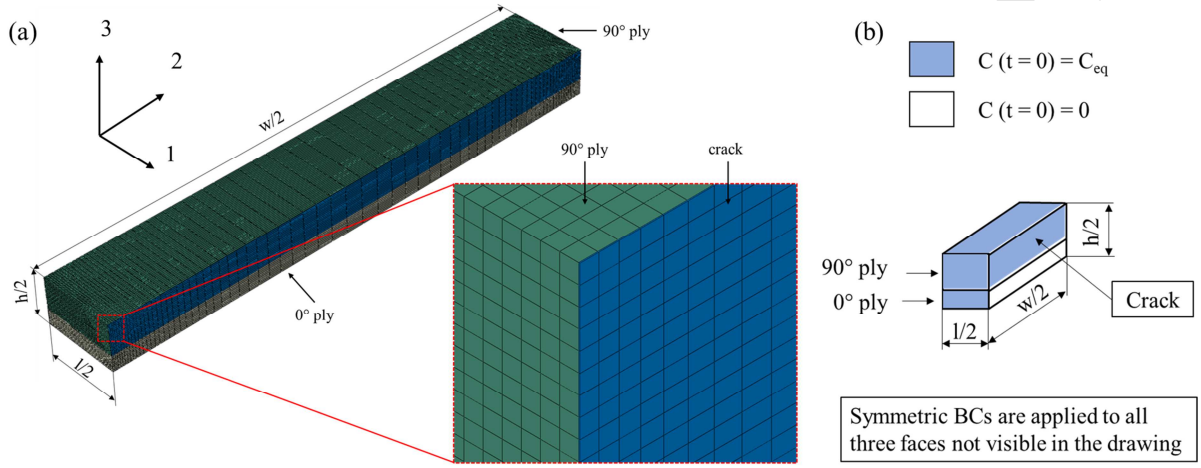

Fig. 9 (a) Example of diffusion FE model for [90/0/90] laminate subjected to ε = 2 % (b) Boundary conditions applied the [90/0/90] laminate

Composite diffusion constant in the axial direction is assumed to be 4.44 times higher than transverse diffusivity, as reported by a previous study of the authors on the same material [3]. Water diffusivity in air is obtained from Hirschfelder-Bird-Sportz equation [16]: 106108 mm^2/h at 60°C.

5. Results and discussion

The weight gain curves of the un-cracked and cracked samples are reported below, **Fig. 10 (a)** for [0/90/0] layup and **Fig. 10 (b)** for [90/0/90] layup.

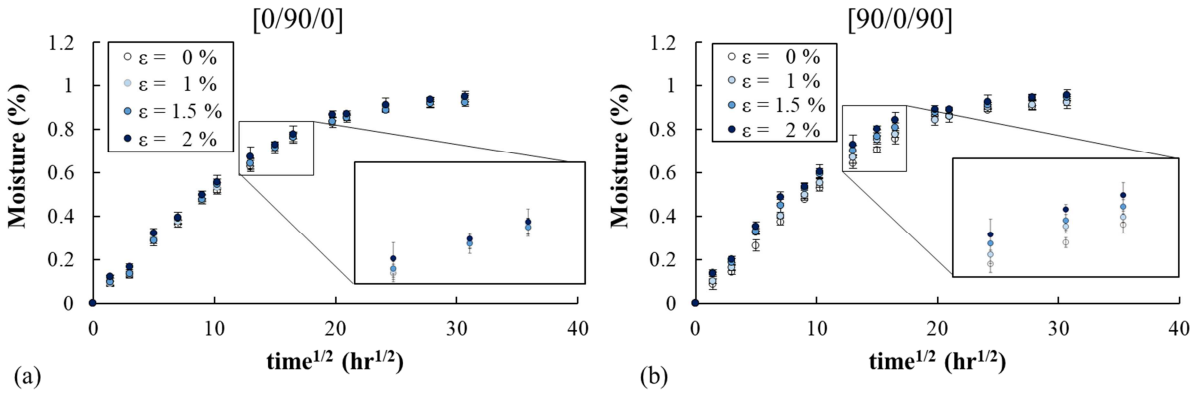

Fig. 10 Weight gain curves for un-cracked samples (ε = 0 %) and cracked samples (ε = 1 %, 1.5 % and 2 %). (a) [0/90/0] lay-up; (b) [90/0/90] layup. Each point is the average of four replicates.

The results of analytical and FE model are compared to the experimental results for both [90/0/90] and [0/90/0] layup in **Fig. 11 (a), (b), (c)** and **(d)**. It is possible to notice that the presence of cracks causes a sensible increase in both diffusivity and moisture saturation content for the [90/0/90] layup.

For the [0/90/0] layup, **Fig. 11 (b)** and **(d)**, the cracks influence on diffusivity and moisture saturation content is negligible, confirming the hypothesis discussed in **Paragraph 3.2**: cracks on the internal plies have a negligible effect in fluid diffusion.

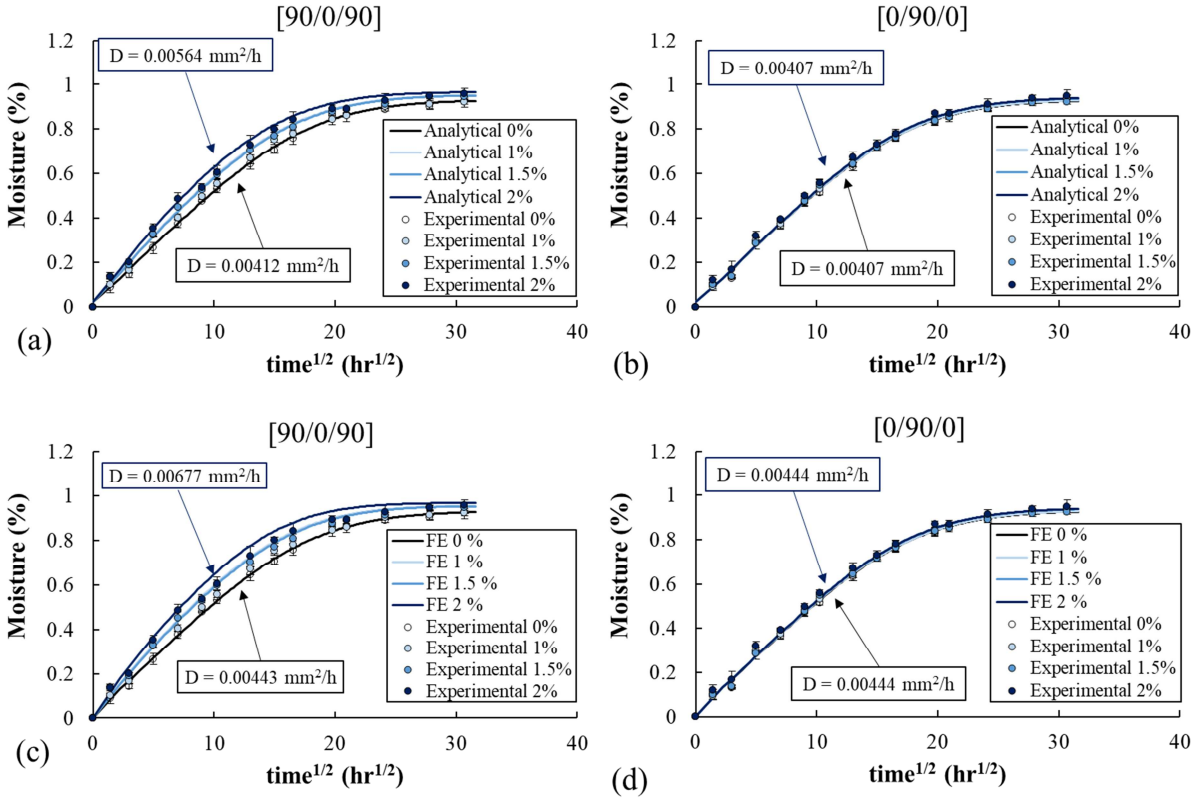

Fig. 11 Weight gain curves for un-cracked samples (ε = 0 %) and cracked samples (ε = 1 %, 1.5 % and 2 %). (a) comparison with analytical model, [90/0/90] layup; (b) comparison with analytical model, [0/90/0] layup; (c)

comparison with FE model, [90/0/90] layup; (d) comparison with FE model, [0/90/0] layup. Each point is the average of four replicates.

The analytical and the FE model show good agreement. The small difference between the two is mainly due to a simplification made in the analytical derivation: the equation used for the weight gain of un-cracked cross-ply laminates, Eq. (20), is based on a weighted average of the diffusivities of each ply, while the FE model considers also the different diffusivity of each ply and the fluid diffusion between the plies in the thickness direction.

The experimental, analytical and FE results are summarized in **Table 4** and **Table 5**.

Table 4
Experimental, numerical and analytical values of apparent diffusion constant

Strain (%)	Experimental (mm^2/h)	Analytical (mm^2/h)	FE (mm^2/h)
0/90/0			
0 %	0.00419	0.00407	0.00444
1 %	0.00443	0.00407	0.00444
1.5 %	0.00463	0.00407	0.00444
2 %	0.00479	0.00407	0.00444
90/0/90			
0 %	0.00443	0.00412	0.00443
1 %	0.00462	0.00500	0.00587
1.5 %	0.00533	0.00491	0.00562
2%	0.00551	0.00564	0.00677

Table 5
Experimental, numerical and analytical values of equilibrium mass increase

Strain (%)	Experimental (%)	Analytical (mm^2/h)	FE (%)
0/90/0			
0 %	0.93	0.930	0.930
1 %	0.94	0.932	0.932
1.5 %	0.94	0.941	0.941
2 %	0.95	0.942	0.942
90/0/90			
0 %	0.93	0.930	0.930
1 %	0.94	0.954	0.954

1.5 %	0.95	0.953	0.952
2%	0.96	0.967	0.968

The analytical and FE model predict the experimental results in terms of moisture equilibrium content very well and in terms of apparent diffusivity a less precisely but still managing to describe the trend. This verifies the validity of hypotheses used in the analytical and FE model:

- The moisture equilibrium content of a cracked composite increases due to the fluid filling the "free volume" created by the cracks;
- Cracks on external plies fill almost immediately with water. This causes an increase in moisture equilibrium content and an increase of diffusivity due to the creation of new surface exposed to water, hence new boundary conditions;
- Cracks on internal plies don't fill immediately with water, being not interconnected in the width direction. This causes still an increase in moisture equilibrium content, but the diffusivity does not increase.
- The assumption of equal distance between the cracks is sufficiently accurate for the model.

The influence of cracks on fluid diffusion in composites has been studied here and validated for a simple case: cross-ply laminates with uniaxial cracks. The analytical solution can be extended to the case of a rectangular shaped RVE having biaxial cracks, like cross-ply laminates having bi-axial cracks or layups containing cracked 45° and -45° plies. This can be done by defining the RVE length and width based on the crack densities of the different plies and changing the diffusion boundary conditions. The numerical FE solution can be extended to arbitrary cracked layups, like laminates containing cracked 60° and -60° plies. In this case it is necessary to define an RVE according to Li *et al.* [17].

This paper has not considered delaminations, which may start from the cracks' tip upon fatigue loading and greatly accelerate diffusivity. The authors are currently working on the extension of this model to the case of laminates having cracks and delaminations.

For offshore and marine applications, thick laminates are often used. Further typical offshore applications such as pipes, hulls and pressure vessels have no free edges exposed to the water. In these structures cracks are likely to have a negligible effect on fluid diffusion.

Conclusions

Based on mono-dimensional fluid diffusion analysis it is shown that cracks on the external layers saturate almost immediately when immersed in water, increasing the initially exposed surface and consequently increasing the speed of water uptake, while cracks in the internal layers do not influence diffusivity, they just increase the fluid saturation content.

An analytical solution for anisotropic fluid diffusion in a cracked laminate is given. This solution is obtained modelling a representative volume element (RVE), whose dimensions are defined by the crack density of the laminate. The diffusion characteristics were also modelled by finite element (FE) analysis, using the same modelling philosophy.

Experiments on glass fiber/epoxy cracked samples confirmed both modelling approaches.

The apparent diffusivity obtained using this model can be used to predict saturation time and concentration profiles for cracked composite structures of arbitrary shape immersed in water.

Acknowledgements

This work is part of the DNV GL led Joint Industry Project "Affordable Composites" with nine industrial partners and the Norwegian University of Science and Technology (NTNU). The authors would like to express their thanks for the financial support by The Research Council of Norway (Project 245606/E30 in the Petromaks 2 programme).

The authors would like to thank also Mr. Emeric Mialon, for the assistance in the samples preparation and testing.

Declaration of interest

None

References

1. Ochoa, O.O. and M.M. Salama, *Offshore composites: Transition barriers to an enabling technology.* Composites Science and Technology, 2005. **65**(15–16): p. 2588-2596.
2. Rocha, I.B.C.M., et al., *Combined experimental/numerical investigation of directional moisture diffusion in glass/epoxy composites.* Composites Science and Technology, 2017. **151**: p. 16-24.
3. Gagani, A., Fan Y., Muliana, A.H., Echtermeyer, A.T. (in press), *Micromechanical modeling of anisotropic water diffusion in glass fiber epoxy reinforced composites.* Journal of Composite Materials, 2017.
4. Roy, S. and T. Bandorawalla, *Modeling of Diffusion in a Micro-Cracked Composite Laminate Using Approximate Solutions.* Journal of Composite Materials, 1999. **33**(10): p. 872-905.
5. Suri, C. and D. Perreux, *The effects of mechanical damage in a glass fibre/epoxy composite on the absorption rate.* Composites Engineering, 1995. **5**(4): p. 415-424.
6. Lundgren, J.-E. and P. Gudmundson, *Moisture absorption in glass-fibre/epoxy laminates with transverse matrix cracks.* Composites Science and Technology, 1999. **59**(13): p. 1983-1991.
7. Perillo, G., N. Vedivik, and A. Echtermeyer, *Damage development in stitch bonded GFRP composite plates under low velocity impact: Experimental and numerical results.* Journal of Composite Materials, 2015. **49**(5): p. 601-615.
8. Carraro, P.A., L. Maragoni, and M. Quaresimin, *Prediction of the crack density evolution in multidirectional laminates under fatigue loadings.* Composites Science and Technology, 2017. **145**: p. 24-39.
9. Roy, S., et al., *Modeling of moisture diffusion in the presence of bi-axial damage in polymer matrix composite laminates.* International Journal of Solids and Structures, 2001. **38**(42–43): p. 7627-7641.
10. M. Dawson, P.D., P. Harper, S. Wilkinson, *Effects of conditioning parameters and test environment on composite materials for marine applications*, in *Durability of Composites in a Marine Environment - 2nd Ifremer ONR Workshop*. 2016: Brest.
11. HEXION, *Technical Data Sheet*, in *EPIKOTE Resin MGS RIMR 135 and EPIKURE Curing Agent MGS RIMH 137* 2006.
12. *Standard Test Method for Moisture Absorption Properties and Equilibrium Conditioning of Polymer Matrix Composite Materials*. 2014, ASTM International.
13. Springer, G., *Environmental Effects on Composite Materials*. Vol. 1. 1984: Technomic Publishing Company.
14. Springer, G., S. Tsai, and G. Springer, *Thermal conductivities of unidirectional materials (Thermal conductivities of unidirectional composite materials parallel and*

normal to filaments, using analogy to shear loading response). JOURNAL OF COMPOSITE MATERIALS, 1967. **1**: p. 166-173.
15. Crank, J., *The mathematics of diffusion*. 1956, Oxford: Clarendon Press.
16. Hirschfelder, J.O., Bird, R.B., Sportz, E.L., *UNIFAC parameter table for prediction of liquid–liquid equilibrium.* Trans ASME, 1949. **71**(921).
17. Li, S., C.V. Singh, and R. Talreja, *A representative volume element based on translational symmetries for FE analysis of cracked laminates with two arrays of cracks.* International Journal of Solids and Structures, 2009. **46**(7–8): p. 1793-1804.

Figure Captions

Fig. 1. Dimensions of the tensile coupons and of the diffusion sample.

Fig. 2. (a) Tensile loading of [0/90/0] sample. (b) Sample before loading. (c) Sample after loading. (d) Cracks are highlighted with red lines. (e) cracks array obtained and used for calculation of ρ_w.

Fig. 3. Crack densities for [0/90/0] and [90/0/90] samples. Each point is the average of 4 measurements

Fig. 4. Optical micrograph of: (a) [0/90/0] cracked sample; (b) [90/0/90] cracked sample.

Fig. 5 Matrix crack in the sectioned 90° ply of a [0/90/0] cracked laminate: (a) Scheme, (b) Section with laminate global coordinate system.

Fig. 6 (a) Optical micrograph of a cracked sample (b) scheme of a non-continuous crack in a [0/90/0] cracked laminate (c) scheme of a non-continuous crack in a [90/0/90] cracked laminate (d) 1-D diffusion model in crack

Fig.7. Laminate dimensions and dimensions of the RVE used for the derivation of the analytical solution

Fig. 8. (a) Scheme of a cracked 90/0/90 laminate (b) RVE for the cracked laminate. (c) 1/8 RVE obtained using 3 symmetry planes. (d) geometry and dimensions of the crack, extending over the whole width of the laminate.

Fig. 9 (a) Example of diffusion FE model for [90/0/90] laminate subjected to $\varepsilon = 2$ % (b) Boundary conditions applied the [90/0/90] laminate

Fig. 10 Weight gain curves for un-cracked samples ($\varepsilon = 0$ %) and cracked samples ($\varepsilon = 1$ %, 1.5 % and 2 %). (a) [0/90/0] lay-up; (b) [90/0/90] layup. Each point is the average of four replicates.

Fig. 11 Weight gain curves for un-cracked samples ($\varepsilon = 0$ %) and cracked samples ($\varepsilon = 1$ %, 1.5 % and 2 %). (a) comparison with analytical model, [90/0/90] layup; (b) comparison with analytical model, [0/90/0] layup; (c) comparison with FE model, [90/0/90] layup; (d) comparison with FE model, [0/90/0] layup. Each point is the average of four replicates.